*Articles*

# X-ray Structures of Recombinant Yeast Cytochrome *c* Peroxidase and Three Heme-Cleft Mutants Prepared by Site-Directed Mutagenesis[†,‡]

Jimin Wang,[§] J. Matthew Mauro,[∥] Steven L. Edwards,[∥] Stuart J. Oatley,[⊥] Laurence A. Fishel, Victor A. Ashford, Nguyen-huu Xuong, and Joseph Kraut*

*Departments of Chemistry, Biology, and Physics, University of California at San Diego, La Jolla, California 92093*

*Received December 27, 1989; Revised Manuscript Received April 5, 1990*

ABSTRACT: The 2.2-Å X-ray structure for CCP(MI), a plasmid-encoded form of *Saccharomyces cerevisiae* cytochrome *c* peroxidase (CCP) expressed in *Escherichia coli* [Fishel, L. A., Villafranca, J. E., Mauro, J. M., & Kraut, J. (1987) *Biochemistry 26*, 351-360], has been solved, together with the structures of three specifically designed single-site heme-cleft mutants. The structure of CCP(MI) was solved by using molecular replacement methods, since its crystals grow differently from the crystals of CCP isolated from bakers' yeast used previously for structural solution. Small distal-side differences between CCP(MI) and bakers' yeast CCP are observed, presumably due to a strain-specific Thr-53 → Ile substitution in CCP(MI). A Trp-51 → Phe mutant remains pentacoordinated and exhibits only minor distal structural adjustments. The observation of a vacant sixth coordination site in this structure differs from the results of solution resonance Raman studies, which predict hexacoordinated high-spin iron [Smulevich, G., Mauro, J. M., Fishel, L. A., English, A. M., Kraut, J., & Spiro, T. G. (1988) *Biochemistry 27*, 5477-5485]. The coordination behavior of this W51F mutant is apparently altered in the presence of a precipitating agent, 30% 2-methyl-2,4-pentanediol. A proximal Trp-191 → Phe mutant that has substantially diminished enzyme activity and altered magnetic properties [Mauro, J. M., Fishel, L. F., Hazzard, J. T., Meyer, T. E., Tollin, G., Cusanovich, M. A., & Kraut, J. (1988) *Biochemistry 27*, 6243-6256] accommodates the substitution by allowing the side chain of Phe-191, together with the segment of backbone to which it is attached, to move toward the heme. This relatively large (ca. 1 Å) local perturbation is accompanied by numerous small adjustments resulting in a slight overall compression of the enzyme's proximal domain; however, the iron coordination sphere is essentially unchanged. This structure rules out a major alteration in protein conformation as a reason for the dramatically decreased activity of the W191F mutant. Changing proximal Asp-235 to Asn results in two significant localized structural changes. First, the heme iron moves toward the porphyrin plane, and distal water 595 now clearly resides in the iron coordination sphere at a distance of 2.0 Å. The observation of hexacoordinated iron for the D235N mutant is in accord with previous resonance Raman results. Second, the indole side chain of Trp-191 has flipped over as a result of the mutation; the tryptophan Nε takes part in a new hydrogen bond with the backbone carbonyl oxygen of Leu-177. From the alteration of local structure that occurs in this mutant, coupled with the results of preliminary functional studies, we infer that Asp-235 exerts influence on the heme iron so as to keep its sixth coordination site vacant, and hence reactive with peroxide substrate, over a wide pH range.

Bakers' yeast mitochondrial cytochrome *c* peroxidase (CCP;[1] ferrocytochrome *c*:$H_2O_2$ oxidoreductase, EC 1.11.1.5) is a monomeric heme-containing 294-residue enzyme (Altschul et al., 1940; Takio et al., 1980; Kaput et al., 1982) that catalyzes the reaction of ferrocytochrome *c* with hydrogen peroxide. A simple conception of the catalytic mechanism includes two stages: (1) an oxidative stage, consisting of peroxide binding and its heterolytic cleavage to form the enzyme intermediate compound I[2] (eq 1.1), and (2) a reductive stage in which two electrons are sequentially delivered by two molecules of ferrocytochrome *c* in order to regenerate the resting-stage enzyme (eqs 1.2 and 1.3) (Yonetani & Ray, 1965, 1966).

$$\text{CCP} + H_2O_2 \rightarrow \text{CMPI} + H_2O \quad (1.1)$$

$$\text{CMPI} + \text{cyt } c^{2+} \rightarrow \text{CMPII} + \text{cyt } c^{3+} \quad (1.2)$$

$$\text{CMPII} + \text{cyt } c^{2+} \rightarrow \text{CCP} + \text{cyt } c^{3+} \quad (1.3)$$

[†] This work was supported by NRSA Postdoctoral Fellowship PHS GM10292-02 to J.M.M., Hemoglobin and Blood Protein Training Fellowship 5 T32 AM07233-11 to L.A.F., NIH Grant RR01644 and a grant from the Markey Charitable Foundation to Ng.-h.X., and NSF Grant DMB 85-11656-01 to J.K. A preliminary account of a portion of this work was previously reported (Mauro et al., 1989).

[‡] Crystallographic coordinates have been submitted to the Brookhaven Protein Data Bank under the entry names 1CCP native, 2CCP mutant D235N, 3CCP mutant W191F, and 4CCP mutant W51F.

* Author to whom correspondence should be addressed.

[§] Present address: Department of Molecular Biophysics and Biochemistry, Yale University, 260 Whitney Ave., New Haven, CT 06511.

[∥] Present address: Center for Advanced Research in Biotechnology, 9600 Gudelsky Dr., Rockville, MD 20850.

[⊥] Deceased April 29, 1988. This work is dedicated to S.J.O., our friend and colleague.

[1] Abbreviations: CCP, cytochrome *c* peroxidase; CCP(MI), recombinant *Escherichia coli* expressed cytochrome *c* peroxidase; CCP(MI,W51F), the Trp-51 → Phe mutant of CCP(MI); CCP(MI,W191F), the Trp-191 → Phe mutant of CCP(MI); CCP(MI,D235N), the Asp-235 → Asn mutant of CCP(MI); EPR, electron paramagnetic resonance; HRP, horseradish peroxidase; metMb, ferric sperm whale myoglobin; MPD, 2-methyl-2,4-pentanediol; *B*-factor, atomic temperature factor.

[2] Compound I is the 2-equiv oxidation product of CCP; compound II is the 1-equiv reaction product of compound I.

0006-2960/90/0429-7160$02.50/0 

From knowledge of the distal heme environment observed in the 2.5-Å X-ray structure of bakers' yeast CCP, Poulos and Kraut (1980a,b) proposed a detailed mechanism for CCP function that included a description of the molecular means of peroxide cleavage and formation of oxidized enzyme intermediates as well as identification of distal tryptophan-51 as the most likely site for the unusual protein-based paramagnetic species observed in the compound I intermediate (Yonetani et al., 1966a; Hoffman et al., 1979; Hori & Yonetani, 1985). The structure of CCP obtained at higher resolution (1.7 Å) (Finzel et al., 1984) revealed additional important details; of particular interest was the observation of favorable hydrogen-bonding distance and geometry between iron-coordinated His-175 and Asp-235 on the heme proximal side. It was proposed that this interaction, which might be expected to result in some degree of deprotonation of the proximal histidine, brings about increased electron density in the His-175 imidazole–Fe–porphyrin system (Finzel et al., 1984; Poulos & Finzel, 1984). It has therefore been asserted that Asp-235 and perhaps other proximal side chains in close proximity to it, notably Trp-191, Met-230, and Met-231, are critical elements of the enzymic machinery responsible for forming or stabilizing the electron-deficient centers that exist in compound I (Edwards et al., 1987).

Despite the detailed three-dimensional picture provided by the refined high-resolution X-ray structure as well as a number of additional biophysical studies of this enzyme, several aspects of the CCP mechanism remain poorly characterized, including the factors controlling substrate binding and heme reactivity, the transition state geometry for peroxide O–O cleavage, the precise chemical nature of compounds I and II, and the pathway(s) of electron transfer from ferrocytochrome *c*.

Recently, site-directed mutagenesis has been used to study CCP [for a review, see Mauro et al. (1989)]. By use of mutant enzymes, new insight has been gained into the spin, coordination, and ligand-binding properties of the heme iron (Smulevich et al., 1988a,b), into the location and chemical characteristics of the paramagnetic center(s) of compound I (Goodin et al., 1986; Fishel et al., 1987; Mauro et al., 1988; Scholes et al., 1989; Sivaraja et al., 1989), and into the elements that control the rate of electron transfer from ferrocytochrome *c* (Miller et al., 1988).

The mutagenesis studies have had the overall aim of systematically examining the ways in which protein architecture is coupled to enzymic function in heme peroxidases. An important part of our work on cytochrome *c* peroxidase consists of accurately assessing any structural changes that occur in mutants having amino acid substitutions at key positions in close proximity to the heme prosthetic group. Therefore, we have determined X-ray structures for a number of crystallized mutants of CCP, each of which was prepared to examine some aspect of enzyme function and each of which has acquired new properties as the result of a single amino acid substitution. The present report describes first the crystal structure of the plasmid-encoded CCP parent enzyme expressed in *Escherichia coli*, CCP(MI), and then comparatively describes structural changes in the following three variants prepared by using site-directed mutagenesis: distal derivative Trp-51 → Phe and proximal derivatives Asp-235 → Asn and Trp-191 → Phe. Finally, since studies describing a number of functional and spectroscopic characteristics of each of these mutants have already been conducted, we discuss each structure in the light of this additional information.

*Crystallization and X-ray Data Collection.* The parent recombinant cytochrome *c* peroxidase, CCP(MI), and the three mutants W51F, W191F, and D235N were expressed in *E. coli* and purified as described previously (Fishel et al., 1987). These four enzymes were crystallized and used for full crystallographic analysis, as described below. In addition, a Ile-53 → Thr mutant was prepared and crystallized in order to investigate the effects of this mutation on crystal packing. For this I53T mutant, only the unit cell dimensions were determined and no further structural work was pursued.

Crystals were grown by mixing protein dissolved to a concentration of approximately 10 mg/mL in 0.10 M potassium phosphate buffer at pH 6.0 with an equal volume (typically 10 μL) of 40% 2-methyl-2,4-pentanediol (MPD)/water (v/v). The 20% MPD/protein solution was then placed as sitting drops on siliconized glass coverslips and equilibrated in sealed dishes against reservoirs containing 30% MPD/water (v/v). Single large crystals were obtained in 3–7 days at 4 °C by seeding with small crystals (Thaller et al., 1981). The initial crystals of CCP(MI) were cross-seeded from bakers' yeast CCP; crystals of the three mutants were grown from seeds of the parent CCP(MI). Crystals of all five proteins were isomorphous within experimental error (space group $P2_12_12_1$; $a$ = 104.9 Å, $b$ = 74.2 Å, and $c$ = 45.5 Å).

Low-resolution X-ray diffraction data for the parent CCP(MI) were initially collected on a CAD4 automatic diffractometer. This data set had an internal agreement $R$-factor of 3.9% among four crystals for intensities of all reflections to 3.5-Å resolution. Higher resolution data (to 2.2 Å) were collected by using the locally developed multiwire area detector diffractometer Mark II system (Xuong et al., 1985a). Each data set was collected by using one crystal at ambient temperature of approximately 23 °C. Area detector data collection was performed according to Xuong et al. (1985b). Crystals were rotated in increments of 0.10 deg/frame around $\omega$ and $\phi$ and $\chi$ angles chosen to sample all unique reflections. Exposure times were approximately 50 s/frame for high-angle detector settings and 20 s/frame at low angle. Approximately 2 days was required to complete intensity measurements for reflections to 2.2-Å resolution for each crystal.

A total of 18 123 unique reflections were collected for CCP(MI), and 17 154, 17 679, and 16 555 unique observations were made for the W51F, W191F, and D235N mutants, respectively. Merging $R_{sym}$[3] values were 4.24, 3.79, 3.58, and 4.25%, respectively, based on an average of 5 observations per unique reflection.

*Initial Structure of CCP(MI) by Molecular Replacement.* The structure of CCP(MI) was solved by the molecular replacement method (Rossmann & Blow, 1962; Crowther, 1972), with the refined structure of bakers' yeast CCP (Finzel et al., 1984) as the search model. Low-resolution CAD4 data were used in rotation function calculations. Rotation angles were sampled at 5-deg intervals, with the best results being obtained with data of 25–4-Å resolution and a vector cutoff of 26 Å. Under these conditions all peaks were 6–8 times above background.

The translation method of Crowther and Blow (1967) was employed to find maximally overlapping intermolecular cross-Patterson vectors between molecules in the model and in the unknown peroxidase structure. Translation functions were calculated by sampling the translation vector on a 1-Å grid, utilizing data between 8.0- and 3.5-Å resolution. Peak-to-noise ratios varied from 9 to 14, with peak half-widths of less than 1 Å. The translation vector was further refined

[3] $R_{sym} = \sum_{hkl}(\sum_i|I_i - \bar{I}|/\sum_i I_i)$, where $I_i$ is the observed intensity of the $i$th reflection and $\bar{I}$ is the scaled mean intensity.

by an *R*-factor minimization procedure with steps of 0.5 Å, resulting in an *R*-factor of 39% for all measurements to 2.2-Å resolution.

*Refinement of the CCP(MI) and Mutant Structures.* The geometry-restrained least-squares method of Hendrickson and Konnert (1980) was used for refinement of the CCP(MI) and mutant structures. The procedure was vectorized on the SDSC CRAY X-MP/48 supercomputer (by S.J.O. and J.W.) to allow refinement of structures having overall thermal anisotropy (Sheriff & Hendrickson, 1987) and to make use of the amorphous solvent correction of Bolin et al. (1982). The overall thermal anisotropy observed in these crystals is characterized by anisotropic lattice disorder, with a larger anisotropic *B*-factor found in the *c* direction in comparison with the other two axes (Wang, 1988). Graphics programs FRODO (Jones, 1978; implemented by S.J.O. on the Silicon Graphics system) and UCSD-MMS (S. Dempsey, unpublished) were used for model manipulation and placement of fixed water molecules.

Two regions within the enzyme molecule where strain-specific primary sequence differences occur between native bakers' yeast CCP and heterologously produced CCP(MI), Asp-152 → Gly and Thr-53 → Ile, were readily observable in both $2F_o$(parent) − $F_c$(model) and $F_o$(parent) − $F_c$(model) maps. During refinement, maps were examined closely after 12 cycles; substitution of Asp-152 by Gly in the CCP(MI) model was made at this stage. Replacement of threonine-53 by isoleucine was made later in the refinement process, because a displacement of His-52 by 0.5 Å was observed, which might have affected the geometry of Ile-53.

Two modifications were introduced in the final stages of refinement of the D235N structure. First, hydrogen atom positions were calculated and their scattering contribution was included in subsequent structure factor calculations. Second, because the *R*-factor was unusually large for reflections below 5 Å, low-order reflections were excluded from subsequent refinement. After additional cycles of refinement, $F_o - F_c$ maps became clearer and more readily interpretable. There were now very few features above $3.5\sigma$, and one of them, at $4.7\sigma$, was close to the initially modeled position of the indole ring of Trp-191. Since this peak was too close to the indole ring to represent an internally bound water molecule, it now seemed that the indole ring must in fact be rotated by about 180°. Reorientation of the ring, followed by further refinement, confirmed this idea. Moreover, the incorrect initial orientation of the indole ring explained why, during the early part of refinement, an unusual distribution of temperature factors was observed for the atoms making up the indole ring.

The refined structure of the CCP(MI) parent included 2382 atoms and 234 ordered water molecules and had an *R*-factor of 15.5%. Overall error was estimated to be approximately 0.17 Å by Luzatti analysis (Luzatti, 1952). The rms deviation of bond lengths from standard values was less than 0.015 Å and the rms deviation from planarity was less than 0.017 Å for each of the four reported structures. Errors in the positions of heme atoms and its neighbors, which have low temperature factors, are probably smaller. Coordinates of CCP(MI) and the W51F, W191F, and D235N mutants refined to $R$ = 15.5, 16.0, 16.5, and 14.7%, respectively, have been deposited in the Brookhaven Protein Data Bank.

Comparison between CCP(MI) and bakers' yeast CCP was made by using a newly refined structure (B. C. Finzel, T. L. Poulos, S. L. Edwards, and J. Kraut, unpublished results) for the latter, in which new 1.7-Å X-ray data were collected on four crystals and the structure was rerefined to $R$ = 17% as compared to 20% previously (Finzel et al., 1984).

*Crystal Packing of CCP(MI).* Although *E. coli* produced CCP(MI) and bakers' yeast CCP crystallize in the same space group, $P2_12_12_1$, the enzyme molecules pack quite differently within their respective crystal lattices. CCP isolated from bakers' yeast has unit cell parameters of $a$ = 107.4 Å, $b$ = 76.8 Å, and $c$ = 51.4 Å, while the unit cell parameters for CCP(MI) are $a$ = 104.9 Å, $b$ = 74.2 Å, and $c$ = 45.5 Å. The unit cell volume for CCP(MI) is thus smaller by approximately 20%, implying a decrease in crystal solvent content of about 50%. In both crystal packing arrangements, the enzyme molecules can be viewed as being assembled into chains running parallel to the *a* axis, with interactions between Glu-221 in the proximal domain of one molecule and Arg-14 in the distal domain of the next molecule linking the chains. In CCP(MI), the intermolecular vectors connecting these residues are tilted about 15° farther away from the *a* axis. The chains therefore pack quite differently in the two crystals, and it follows that all other intermolecular interactions differ as well.

The reason for the difference in crystal packing between CCP(MI) and CCP isolated from bakers' yeast is still unclear. Of the two strain-specific amino acid differences between the two enzymes (Kaput et al., 1982), Thr-53 and Asp-152 in bakers' yeast CCP versus Ile-53 and Gly-152 in CCP(MI), the present results rule out the substitution at position 53 as being responsible for the difference in crystallization behavior, since the Thr-53 mutant of CCP(MI) crystallized isomorphously with the parent. The Asp → Gly substitution at position 152, which lies on the enzyme surface, must still be considered a possible reason for the observed crystal packing difference. The replacement of the aspartate in the enzyme isolated from commercial bakers' yeast by glycine in CCP(MI) undoubtedly alters the local charge distribution of the enzyme surface. However, this region of the protein faces a solvent channel in both crystal forms and does not engage in any direct intermolecular contacts with adjacent peroxidase molecules. Therefore, it is not obvious how the substitution at position 152 could result in the observed crystal packing effect.

Conceivably, the Met-Ile dipeptide fused to the N-terminus of plasmid-encoded CCP(MI) may be responsible for the difference in crystal packing; however, it is noted that neither these two residues nor the next two (Thr-1 and Thr-2) were visible in the final electron density map, and even the succeeding two residues had exceptionally large temperature factors (more than 70 Å$^2$). A similarly high mobility of the N-terminal residues was observed in the high-resolution (1.7-Å) refined bakers' yeast CCP structure (Finzel et al., 1984). These N-terminal residues also face a solvent channel in both of the crystal packing arrangements, and the lack of any direct intermolecular interactions in the crystal lattice again makes it impossible to assign the present crystal packing differences as being simply due to different N-termini in the two enzymes. Other conceivable explanations include the possibility that more significant differences between the enzyme as isolated from bakers' yeast and from *E. coli* occur as a result of protease action in vivo or during purification or that other posttranslational modifications such as deamidation of Asn or Gln residues occur, which subsequently affect crystallization.

*Structural Comparison of CCP(MI) and Bakers' Yeast CCP.* Structural features making up the heme cleft of CCP(MI) that are most relevant to the present work are shown in Figure 1a. The refined structure of CCP(MI) is nearly identical with that of bakers' yeast CCP. However, some subtle differences around the peroxide-binding pocket on the

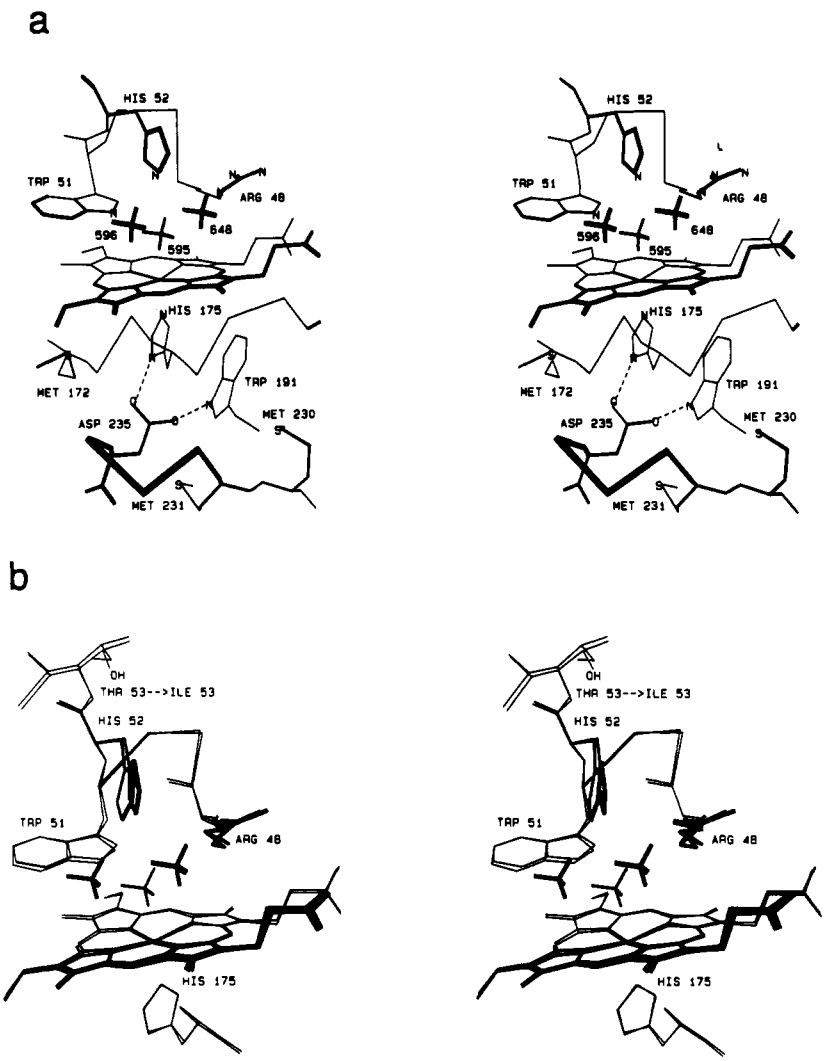


FIGURE 1: (a) The heme cleft of CCP(MI). Some important hydrogen-bonding interactions are indicated by dashed lines. Trp-51, Trp-191, and Asp-235, the sites of the mutations described in the text, are labeled, along with several other important side chains. The positions of water molecules 595, 596, and 648 are also shown. (b) Superposition of bakers' yeast CCP and CCP(MI) structures, showing the difference in His-52 positions and the strain-specific Thr-53 → Ile substitution. See (a) for water molecule numbering. The bakers' yeast CCP coordinates are from the Brookhaven Protein Data Bank (B. C. Finzel, T. L. Poulos, and J. Kraut, April 1986).

heme distal side were observed (Figure 1b). The most significant structural difference between the bakers' yeast enzyme and CCP(MI) occurs in the region of distal His-52. In the former molecule, the imidazole ring of His-52 is tilted with respect to the heme axis so that it appears to be nearly ideally hydrogen-bonded to Wat-596, which lies between pseudoaxial Wat-595 and Nε of Trp-51. In CCP(MI), the imidazole of His-52 is more nearly axially positioned with respect to the heme iron, the end of the five-membered ring having swung approximately 0.5 Å toward the axis through the iron perpendicular to the porphyrin plane. Perhaps as a consequence of improved hydrogen-bonding geometry resulting from the reorientation of His-52, Wat-595 moves away from the iron atom and closer to Nε of the histidine; the new distance between Wat-595 and the heme iron is 2.7 Å in CCP(MI) compared with 2.4 Å in bakers' yeast CCP. A typical ferric heme iron-to-water ligand distance is 1.9–2.1 Å (Scheidt & Gouterman, 1983); therefore, we conclude that the iron in CCP(MI) remains in a pure pentacoordinated state in which Wat-595 is even more effectively kept away from the iron than in the enzyme isolated from commercial bakers' yeast by means of its improved interaction with a slightly reoriented His-52.

Evidently the small positional adjustments of His-52 and Wat-595 are due to the strain-specific Thr-53 → Ile substitution in CCP(MI). In bakers' yeast CCP, Oδ1 of Thr-53, which is near the C-terminal end of distal helix B, hydrogen bonds to the backbone carbonyl oxygen of a leucine residue (Leu-49) that lies approximately in the middle of the same helix. Oγ1 of Thr-53 is also hydrogen-bonded to two interior water molecules that are not present in CCP(MI). It is likely that helix B, from which His-52 projects toward the heme, is flexed slightly differently in the two molecules as a result of the differing internal interactions around residue 53. Unfortunately, in the case of the present nonisomorphous crystal forms we cannot examine these subtle changes by using difference Fourier maps, which are more sensitive to small changes than is comparison of coordinates derived by least-squares refinement.

Of the 234 ordered water molecules that were assigned positions in the CCP(MI) structure, about 130 are in the same locations relative to the enzyme molecule as found in the bakers' yeast CCP structure (Finzel et al., 1984). The average isotropic temperature factor, $B$, for fixed water molecules is 58 Å$^2$. Three internal water molecules near the iron atom, Wat-595 (which lies closest to the iron), Wat-596, and Wat-648, have temperature factors approximately twice as large as the values for the corresponding water molecules in bakers' yeast CCP. The $B$-factors are 40, 58, and 57 Å$^2$ for Wat-595, Wat-596, and Wat-648, respectively, in CCP(MI).

These changes in thermal parameters are probably also due to the replacement of Thr-53 by Ile in CCP(MI). Interestingly, the temperature factors for these distal-side fixed water molecules are also affected by the *proximal* Asp-235 → Asn mutation described below.

Examination of the enzymic and spectroscopic properties of CCP(MI) compared with those of bakers' yeast CCP has revealed no gross differences (Fishel et al., 1987; Mauro et al., 1988; Scholes et al., 1989), but more careful study may well show subtle effects.

*Spectral and Kinetic Properties of CCP(MI,W51F).* The indole ring of Trp-51 lies 3.3 Å above heme pyrrole rings I and II and approximately parallel to the porphyrin plane and forms an interior boundary of the pocket into which peroxide substrate must enter in order to bind at the sixth iron coordination site. It is also potentially positioned to influence the chemistry of the heme through $\pi$–$\pi$ interactions with the porphyrin macrocycle as well as through hydrogen-bonding interactions with iron-bound ligands. Due to its placement with respect to the heme, Trp-51 was initially proposed as the most probable locus of the non-heme paramagnetic center in compound I of CCP (Poulos & Kraut, 1980a). The analogous site is occupied by phenylalanine in catalase (Murthy et al., 1981), HRP (Welinder, 1976), turnip isoperoxidases (Welinder & Mazza, 1977; Mazza & Welinder, 1980), and ligninase (Tien & Tu, 1987), and none of these heme enzymes exhibits EPR behavior resembling that of compound I of CCP. A W51F mutant of CCP(MI) was therefore prepared and characterized in some detail (Fishel et al., 1987) in order to ascertain whether substitution at this site by phenylalanine would abolish the unusual paramagnetic center.

It has now been established that the characteristic axially symmetric signal observed in the 4 K EPR spectrum of the peroxide-oxidized W51F mutant is essentially unchanged from the signal observed for compound I of the parent enzyme, a finding which strongly suggests that the paramagnetic center of compound I is not located at Trp-51 (Goodin et al., 1987; Scholes et al., 1989). In fact, evidence has now been accumulated indicating that the protein-based paramagnetic species in compound I *is* associated with a tryptophan side chain, most probably proximal Trp-191 (Mauro et al., 1988; Scholes et al., 1989; Sivaraja et al., 1989). Nevertheless, some significant changes in the properties of the enzyme have resulted from the Trp → Phe mutation at position 51, including the following: (1) Resonance Raman spectra of ferric CCP(MI) indicate that the heme iron of the parent exists mainly in the *pentacoordinate* high-spin state in solution at neutral pH, whereas CCP(MI,W51F) exists in the *hexacoordinate* high-spin state under the same solution conditions (Smulevich et al., 1988a). (2) The pH and temperature dependencies of the spin of the ferric iron in resting-state CCP(MI,W51F) are perturbed, as demonstrated by the 90 K EPR spectrum for the mutant at pH 6 (Fishel et al., 1987). (3) The half-lives of spontaneous decay of the protein-associated paramagnetic species and the oxyferryl center in the peroxide-oxidized mutant enzyme (in the absence of ferrocytochrome *c*) are decreased by about 70-fold in the mutant (Fishel et al., 1987). (4) Although the mutant enzyme remains extremely active in its role of promoting reaction between hydrogen peroxide and ferrocytochrome *c*, its steady-state kinetic parameters are clearly different from those of the parent enzyme. The pH of maximum substrate turnover for both bakers' yeast CCP and CCP(MI) is about 5, whereas it is about 6.5 for CCP(MI,W51F) (Goodin et al., 1987). Furthermore, when the activities of the parent and the mutant enzyme were compared at pH 6, it was found that $k_{cat}$ for the mutant is increased by a factor of 2–3, but $K_m$ values for both hydrogen peroxide and ferrocytochrome *c* are slightly increased as well (Fishel et al., 1987; Goodin et al., 1987). (5) Resonance Raman spectra recorded for the mutant immediately after mixing with hydrogen peroxide (before rapid spontaneous decay of the oxyferryl center occurs) show that its Fe(IV)=O stretching frequency is upshifted by 25–30 $cm^{-1}$ compared to the stretching frequency of the oxyferryl group of compound I of CCP(MI). In fact, the Fe(IV)=O stretching frequency measured for the oxidized mutant closely approximates the analogous Fe(IV)=O stretching frequency for compound II of HRP (J. Terner, unpublished results).

*Crystal Structure of CCP(MI,W51F).* A difference Fourier map, $F_o$(W51F) – $F_o$(parent), superimposed on a model of the parent CCP(MI) structure in the region of the mutation is shown in Figure 2a. The map was very clear, with significant density (>4$\sigma$) occurring only in the vicinity of the Trp → Phe side-chain substitution and near the backbone and side-chain atoms of helix B, the helix from which the catalytically important residues His-52 and Arg-48 as well as Trp-51 (or Phe-51) project. The most prominent difference features (−15$\sigma$ and +10$\sigma$) appeared near the indole ring of Trp-51 of the superimposed parent structure and were consistent with the absence of the five-membered portion of the indole ring system in the mutant. The second largest positive peak (6$\sigma$) in the difference map was observed below (that is, toward the heme plane) the imidazole ring of His-52. This difference density feature, along with the presence of a number of positive peaks below and negative peaks above the residues making up helix B, immediately suggested that a small overall movement of this helix toward the heme had occurred. Additional distal-side difference density was evidently due to changes in temperature factors and/or occupancies of the ordered water molecules bound in the distal heme cavity. In particular, the site of Wat-648 is much less occupied, or perhaps completely missing, in this mutant, whereas a positive peak, of about 4$\sigma$ in intensity, suggested that Wat-595 either is more ordered or has a higher occupancy in CCP(MI,W51F) than in the parent CCP(MI).

The initial model for crystallographic refinement of the W51F mutant was obtained by inspecting the $2F_o$(W51F) – $F_o$(parent) map in order to position the side chain of phenylalanine-51. After least-squares refinement, comparison of the mutant and parent structures showed that C$\beta$ of phenylalanine-51 was laterally displaced about 0.5 Å compared to the C$\beta$ group of tryptophan-51 in the parent enzyme (Figure 2b). The Phe-51 phenyl ring occupies approximately the same plane with respect to the heme as the indole ring of the parent but is now located so that the centroid of its six-membered ring approximately superimposes with the centroid of the position previously occupied by the nine-membered indole ring. The small backbone adjustment necessary to allow this position of the phenylalanine side chain is best described as a generalized diagonal displacement of residues 48–53 of distal helix B. This small displacement toward the heme, by an average of 0.3 Å for residues 48–53, results in a slightly smaller peroxide-binding cavity in the mutant enzyme.

The position and high occupancy of distal fixed water 595 in the refined mutant structure suggest that distance and geometry criteria are fulfilled for good hydrogen bonding between this water molecule and side-chain nitrogen atoms contributed by nearby Arg-48 and His-52. Apparently as a result of these interactions, Wat-595 in the crystallized mutant enzyme remains centered 2.7 Å from the heme iron even

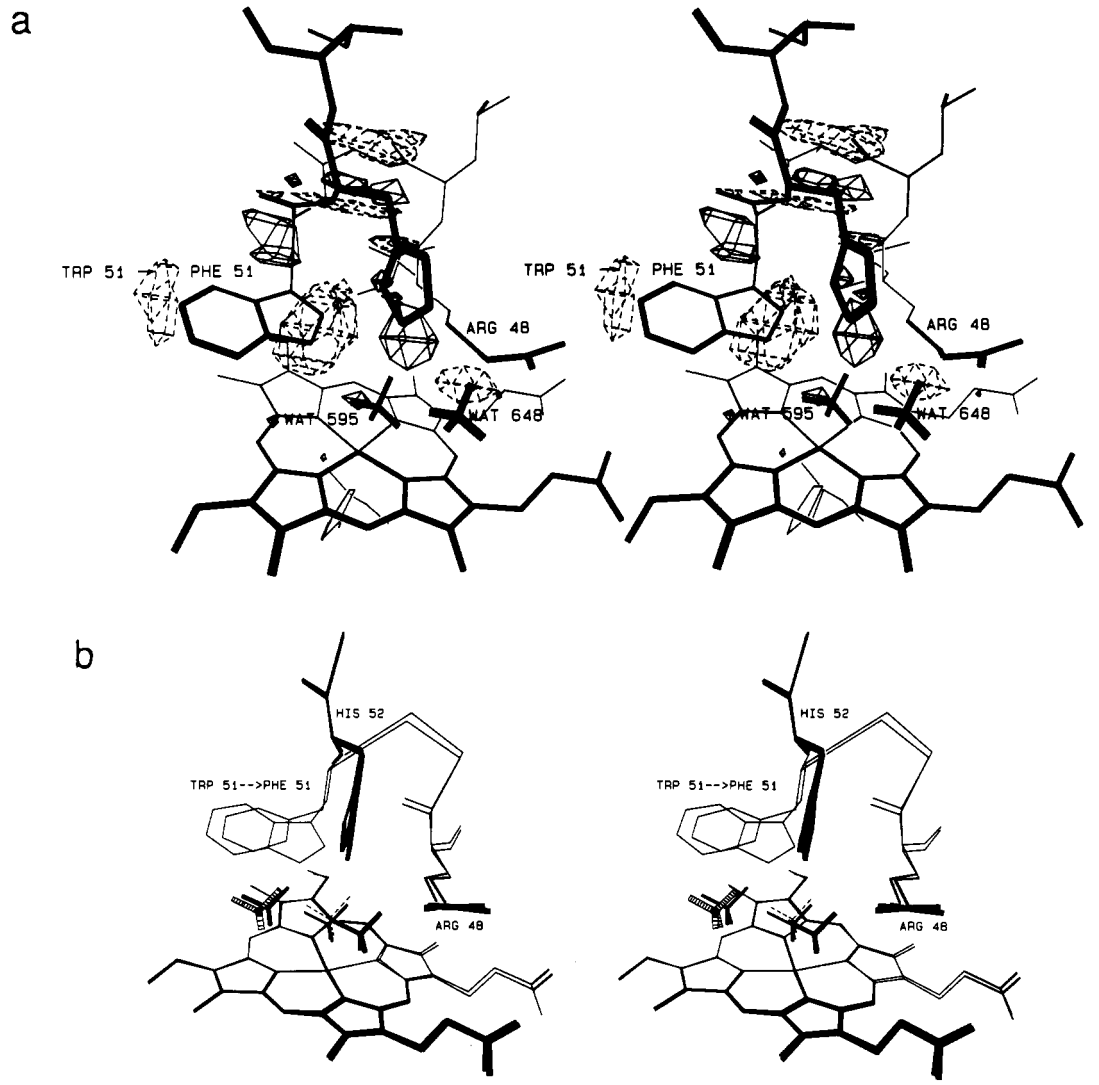


FIGURE 2: (a) CCP(MI,W51F) minus CCP(MI) difference Fourier map contoured at $\pm 5\sigma$. Dashed contour lines represent negative difference density; solid lines represent positive difference density. (b) Superposition of refined structures of CCP(MI,W51F) and CCP(MI). Water molecules 595/596 of the W51F mutant are shown dashed/striped. See Figure 1a for water molecule numbering.

though it now lacks the hydrogen bond it previously made with N$\epsilon$ of Trp-51. Since this Fe–$H_2O$ distance differs little if any from that of the parent, we conclude that the iron remains essentially pentacoordinated in the W51F mutant as crystallized from 30% MPD. In addition, fixed water 596 has moved approximately 1 Å away from the side chain at position 51 relative to its position in the parent (Figure 2b). Finally, the present model for CCP(MI,W51F) has no water molecule in or near position 648, since we could not confidently assign the weak electron density in this region to a water molecule.

The observation of pentacoordinate iron in the crystal structure of CCP(MI,W51F) differs from the results of resonance Raman studies conducted on the mutant enzyme in solution (Smulevich et al., 1988a). On the basis of the characteristic $\nu_3$ band frequency at 1483 $cm^{-1}$ for hexacoordinate high-spin iron, the spectroscopic results indicated that the ferric heme in this mutant peroxidase is almost completely hexacoordinated at pH 6, where crystals used for X-ray data collection were grown. Additional resonance Raman work by Smulevich et al. (1990) indicates that adding concentrations of 2-methyl-2,4-pentanediol (MPD) necessary to induce crystallization (30% v/v) results in a hexa- to pentacoordinate change in iron coordination state for this mutant. The coordination state of parent CCP(MI) is not significantly altered by adding MPD, and of the mutants thus far examined, this behavior has been observed to a significant degree only with the F51 mutant. It appears that replacement of the indole ring of distal Trp-51 with a phenyl group, which is smaller and also incapable of hydrogen bonding with Wat-595, renders the enzyme's distal side unique susceptible to minor structural changes brought about by MPD, which ultimately affect the iron coordination state. We stress, however, that in none of the presently described structures, including CCP(MI,W51F), is there electron density recognizable as being due to ordered MPD either in the distal heme pocket or anywhere else in the molecule. Therefore, we surmise that the effect of MPD on the W51F mutant's iron coordination state is probably due to propagation of subtle structural changes to the heme center rather than due to the presence of MPD bound within the polar distal cavity of the enzyme. Nonetheless, these results demonstrate that X-ray crystallography and resonance Raman spectroscopy each provides a consistent view of the iron coordination state when the experimental conditions are properly controlled. However, the changed coordination behavior exhibited by CCP(MI,W51F) under the conditions necessary for its crystallization illustrates the delicacy of the structural balance that determines the coordination state of the ferric iron in this mutant.

In light of the relatively minor adjustments that take place in the positions of the catalytically involved distal side chains

of His-52 and Arg-48 as a result of the Trp-51 → Phe mutation, it is not surprising that the mutant enzyme remains fully active (Fishel et al., 1987). The reason for the substantial change in pH optimum for steady-state performance reported for this mutant by Goodin et al. (1987) remains unexplained, however, and the present structure affords no simple explanation for this phenomenon.

The absence of any large structural adjustments of distal helix B in the W51F mutant leads us to conclude that the 25–30-$cm^{-1}$ upshift in Fe(IV)=O stretching frequency for compound I of the W51F mutant compared with the analogous frequency for compound I of parent CCP(MI) (J. Terner, unpublished results) is due solely to differing interactions between Trp versus Phe at position 51 and the oxyferryl oxygen or the heme $\pi$-electron system. It is most likely that the significant upshift in Fe(IV)=O stretching frequency, which implies a shorter, stronger iron–oxygen bond in the peroxide-oxidized W51F mutant, results from the loss of the hydrogen bond between the iron-bound oxo group and N$\epsilon$ of Trp-51 that exists in the oxyferryl parent enzyme. It cannot be ruled out, however, that differences in charge-donating ability of tryptophan compared to phenylalanine also affect the properties of the oxyferryl center, since on the basis of NMR studies Satterlee et al. (1983) have proposed that increased charge density on heme pyrrole II resulting from its interaction with Trp-51 ultimately affects the heme iron by enhancing porphyrin → Fe $\pi$ donation. Changes in H-bonding interactions, charge donation, or both presumably also contribute to the 70-fold increase in the rate of spontaneous reduction of the oxyferryl center of peroxide-oxidized CCP(MI,W51F) by some unknown endogenous electron donor (Fishel et al., 1987).

The Trp → Phe mutation at position 51 of CCP(MI) results in a primary sequence for distal helix B (R48-L49-A50-F51-H52-I53) that now even more closely resembles the already highly homologous (R38-L39-H40-F41-H52-D53) corresponding region of HRP. The aligned sequences indicate that HRP has a phenylalanine (F41) in a position analogous to phenylalanine-51 of CCP (MI,W51F) (Welinder, 1976). In addition, the Fe(IV)=O stretching frequency of approximately 780 $cm^{-1}$ observed for the W51F mutant closely approximates the 788-$cm^{-1}$ Fe(IV)=O frequency of compound II of alkaline HRP (Sitter et al., 1985). This similarity, coupled with the sequence identity between distal helix B of the W51F mutant of CCP(MI) and HRP, indicates that the structure of the mutant in this localized region may be a reasonably good model for the region around phenylalanine-41 in the plant peroxidase. The availability of this mutant, together with its structure, should be useful in the interpretation of the results of magnetic resonance studies, where inversion of the positions of the proton chemical shifts of heme 3- and 8-methyl groups of the porphyrin ring in CCP compared to HRP has been proposed to result from the difference in charge-donating ability of tryptophan compared to that of phenylalanine at position 51(41) (Satterlee et al., 1983).

*Properties of CCP(MI,W191F).* Tryptophan-191 projects off the end of a relatively flexible loop on the proximal side of the heme in such a way that its indole ring lies parallel to and in van der Waals contact with the iron-coordinated proximal imidazole of His-175. The indole also makes contact with the porphyrin ring at the bridging $\gamma$-methylene group between pyrrole rings III and IV (Figure 1a). In addition, an indirect hydrogen-bonded linkage between the proximal imidazole and the indole of Trp-191 is provided by the side chain of Asp-235, which makes hydrogen bonds with both N$\delta$1 of His-175 and N$\epsilon$ of Trp-191. The unusual positioning of Trp-191 was initially noted by Poulos and Finzel (1984) in a discussion of the CCP X-ray structure. This side chain was considered as a candidate for the locus of the non-heme paramagnetic center of compound I after mutagenesis experiments ruled out two more obvious sites, Trp-51 and Met-172 (Goodin et al., 1986, 1987; Fishel et al., 1987). Additionally, an X-ray difference Fourier study suggested that small structural perturbations occur on the proximal side of the heme in the vicinity of Trp-191 upon formation of compound I (Edwards et al., 1987).

On the basis of the above considerations, it seemed possible that Trp-191 might be important in formation or stabilization of the oxyferryl heme and/or the unusual protein-based radical species observed in compound I. Since replacement of this residue by phenylalanine should disrupt critical proximal-side $\pi$-orbital interactions and hydrogen bonds while causing minimal overall structural disturbance, it was expected that examination of the characteristics of this variant might yield important structural and functional information about the CCP molecule. Indeed, significant changes in the kinetics of both compound I formation and electron transfer from ferrocytochrome *c* to the $H_2O_2$-oxidized enzyme occur as a result of this Trp → Phe substitution. The effect on electron transfer is very large and evidently accounts for the approximately 3000-fold diminution in the steady-state rate of hydrogen peroxide dependent oxidation of ferrocytochrome *c* catalyzed by the W191F mutant as compared to parent CCP(MI) (Mauro et al., 1988). The impairment of electron transfer capability that occurs as a result of the mutation is especially intriguing, since the integrity of the oxyferryl center and formation of the complex between the enzyme and cytochrome *c* appear to be relatively unaffected.

It has been proposed that the enzymic process leading to formation of 2-equiv-oxidized compound I of CCP proceeds by means of a transient intermediate containing a porphyrin $\pi$-cation radical species (Chance et al., 1967) that rapidly breaks down by oxidation of some nearby amino acid residue or residues (Chance et al., 1986). This hypothesis has been difficult to investigate, since porphyrin $\pi$-cation radical breakdown may occur so rapidly that this intermediate is not observable by presently available stopped-flow techniques. However, fast spectral scanning stopped-flow examination of rapidly mixed solutions of hydrogen peroxide and CCP(MI,W191F) shows that an initial intermediate is formed that has the visible spectrum expected for a porphyrin $\pi$-cation radical (Erman et al., 1989). Furthermore, the rate of reaction of the mutant enzyme with $H_2O_2$ becomes independent of peroxide concentration at low concentrations of the oxidant, unlike the parent peroxidase/peroxide reaction, which remains first order for both reactants over a wide range of concentrations. These experiments suggest that the W191F mutant's reaction with peroxide proceeds by formation of a porphyrin $\pi$-cation radical whose relatively slow breakdown by an endogenous reduction reaction is rate-limiting. Thus, the Trp → Phe substitution at position 191 has resulted in very significant functional changes both in the initial stage leading to the formation of an oxidized intermediate and in the subsequent reductive stage requiring electron transfer from ferrocytochrome *c*.

The EPR spectrum of compound I of CCP(MI) at 4 K reveals two components: a highly temperature-dependent axial signal, which is the major integrated spin contributor, and a superimposed narrow, substoichiometric isotropic feature resembling an organic radical signal. Comparison of 4 K EPR

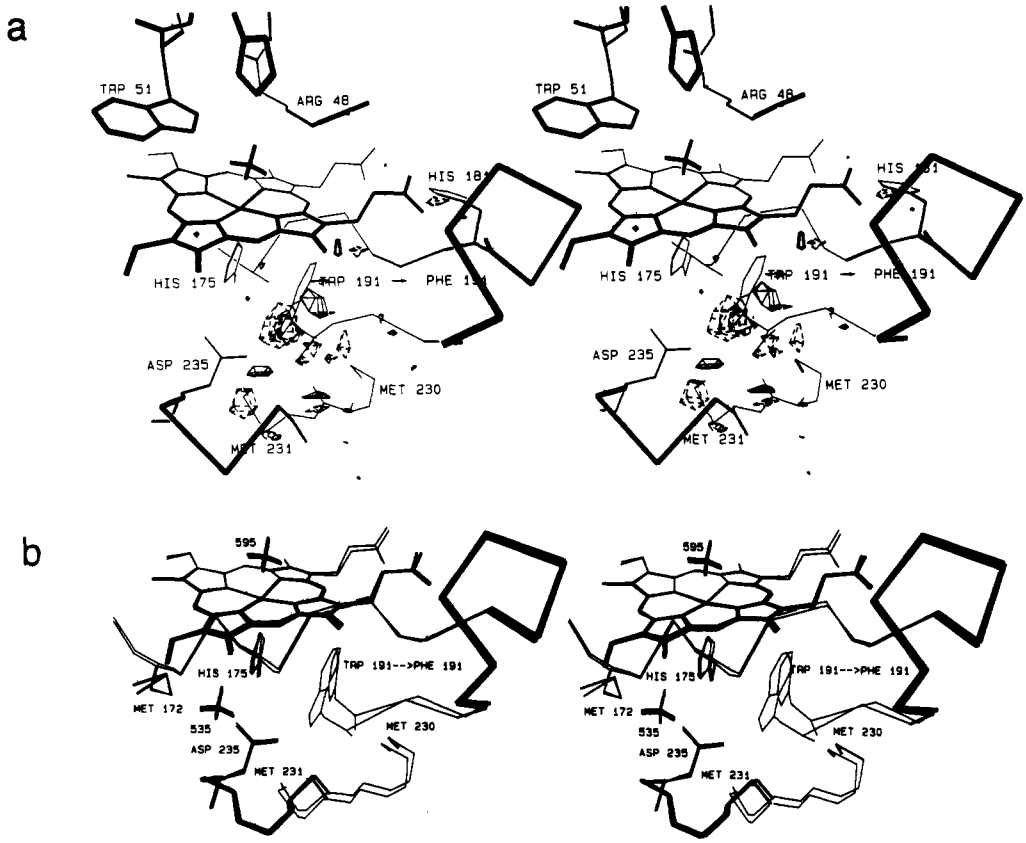


FIGURE 3: (a) CCP(MI,W191F) minus CCP(MI) difference Fourier map contoured at $\pm 5\sigma$. (b) Superposition of refined structures of CCP(MI,W191F) and CCP(MI).

spectra of compound I of the parent CCP(MI) and of peroxide-oxidized CCP(MI,W191F) clearly showed that the dominant axial signal was not present in the 4 K EPR spectrum of the oxidized mutant enzyme (Scholes et al., 1989), indicating that the mutation very likely eliminated the site of the stable radical in compound I. Concurrent with those experiments, Sivaraja et al. (1989) isolated CCP containing perdeuterated tryptophan from an *E. coli* tryptophan auxotroph and performed ENDOR studies confirming that a tryptophan is responsible for the dominant axial EPR signal. Although the above evidence suggests the possibility of a connection between the dramatic decrease in catalytic competence of the phenylalanine-191-substituted enzyme and loss of the ability of the enzyme to form the paramagnetic species characteristic of compound I, no conclusive proof exists that the ability to form a *radical* at Trp-191 is necessary for efficient functioning of CCP. However, the presence of Trp-191 is evidently necessary for efficient electron transfer from cytochrome *c* to occur.

The dramatic effects of this single substitution on the catalytic function and magnetic properties of the enzyme made it desirable to obtain a detailed view of its three-dimensional structure. The crystallographic analysis described below shows that no large structural perturbations result from the Trp-191 → Phe mutation.

*Crystal Structure of CCP(MI,W191F).* The W191F mutant crystal structure revealed small but more widely distributed perturbations than were seen for the W51F mutant, as indicated by the 2-fold increase in overall root-mean-square difference density in the $F_o$(W191F) − $F_o$(parent) difference Fourier map compared to the $F_o$(W51F) − $F_o$(parent) map. Contoured at the $5\sigma$ level, the W191F map showed that the major differences were located entirely within the proximal domain (Figure 3a). As expected, the largest features, $-9.1\sigma$ and $+7.4\sigma$, were located at residue 191, near the former position of the five-membered ring of the parent's Trp-191 side chain, and in the immediately surrounding region. At a lower contour level, $\pm 3\sigma$, it was found that almost all the proximal atoms of the molecule had positive difference density above and negative density below (in the orientation of Figure 3a), suggesting that a small widespread structural adjustment occurs in the proximal hemisphere of the mutant.

Least-squares refinement was initiated by modeling the side chain of Phe-191 on the basis of the $2F_o$(W191F) − $F_o$(parent) map. After refinement, it was apparent that all significant structural adjustments occur on the heme proximal side; the root-mean-square magnitude of the movements is 0.14 Å. The largest adjustment is a 1.0-Å movement by Cα of Phe-191 toward heme pyrrole ring I (Figure 3b) so that its phenyl ring is located virtually coincident with the position of the six-membered portion of the indole ring of the parent peroxidase. This relatively large movement is apparently tied to other changes in the proximal domain through backbone hydrogen bonds between five antiparallel extended strands, of which the topmost strand contains residue 191. This five-stranded structure composes a large part of the proximal domain, and it moves in concert with Cα of Phe-191; thus, much of the proximal domain is slightly compressed toward the heme. Coincident with this small (average 0.3 Å) compressive adjustment in the proximal domain is a slight expansion in the extended-strand direction. The net result is a damping out of the overall structural perturbation introduced by the defect at position 191 by means of a large number of small protein adjustments distributed over a wide region of the proximal domain.

On the basis of the present 2.2-Å structure, it appears that the iron coordination sphere and the geometry of Asp-235 and His-175 are relatively unaffected by the Trp-191 → Phe

mutation, although an angular rotation of the proximal histidine of less than about 10° would not be accurately observable at the present resolution. This finding is supported by spectroscopic work, which has been aimed at probing the heme microenvironment in this mutant. Thus, in the resting state at pH 6, and UV–visible spectrum and the high-frequency resonance Raman spectrum of ferric CCP(MI,W191F) are very similar to those of the parent CCP(MI) (Mauro et al., 1988; Smulevich et al., 1988a) and indicate that the mutated enzyme still contains mainly pentacoordinated high-spin ferric iron. Additional resonance Raman analysis of the peroxide-oxidized mutant enzyme shows that its Fe(IV)=O stretching frequency is essentially identical with that of compound I of CCP(MI), an observation which further suggests that iron–porphyrin–ligand interactions are not seriously altered in the mutant (J. Terner, unpublished observations). Finally, the ferric/ferrous midpoint potential at pH 7 for the mutant is −202 mV, compared to a value of −194 mV determined for the parent, indicating that no large change in the relative stabilities of these two redox forms occurs as a result of the mutation (Mauro et al., 1988).

We previously proposed that the new and significantly different properties of the W191F mutant are probably due to localized effects resulting from the amino acid replacement rather than due to gross structural perturbations (Mauro et al., 1988). Unless the enzymic function of CCP is extraordinarily sensitive to the small adjustments in the proximal domain just described, we believe that the present mutant X-ray structure provides strong additional support for the previous conclusions. Thus, the most probable reasons for the diminished ability of the Fe(IV)=O center to accept electrons from ferrocytochrome *c* are either that the reorganization energy necessary to allow the oxidized iron center to achieve the transition state required for electron transfer is significantly increased in the mutant or that the indole ring of Trp-191 is an important element in an intermolecular electron transfer pathway.

*Properties of CCP(MI,D235N).* In both bakers' yeast CCP and CCP(MI), the carboxyl oxygen atoms of Asp-235 are the central elements in a hydrogen-bonded assembly involving Nδ1 of the proximal imidazole of His-175 and Nε of the indole ring of Trp-191 (Figure 1a). This set of interactions is unique among heme proteins of known tertiary structure, although a similar proximal-side apparatus may well exist in other peroxidases (Poulos & Finzel, 1984). Distance and angle information garnered from the 1.7-Å X-ray crystal structure of cytochrome *c* peroxidase (Finzel et al., 1984) suggest that a strong hydrogen-bonding interaction between Nδ1 of proximal His175 and Oδ1 of Asp-235 occurs in the parent enzyme. Furthermore, Raman observations of the resonance-enhanced iron–Nε (imidazole) stretching frequency of the Fe(II) enzyme suggest that the participating hydrogen is at least partially transferred to Oδ1 of Asp-235 so that the imidazole of His-175 exists largely in a deprotonated, imidazolate form (Stein et al., 1980; Teraoka & Kitagawa, 1981). It has been proposed that this H-bonding interaction between the proximal histidine and the carboxylate of Asp-235 acts to stabilize the high oxidation state [Fe(IV)] of compound I (Finzel et al., 1984) by enhancing the anionic character of the enzyme's iron–porphyrin system. In order to probe this purported functional role of Asp-235, we have replaced it with Asn by using site-directed mutagenesis.

Resonance Raman experiments designed to investigate heme spin and coordination behavior for the D235N mutant were carried out concurrently with the present X-ray crystallographic work (Smulevich et al., 1988a). These studies strongly suggested that replacement of Asp-235 by Asn significantly perturbs the protonation state of Nδ1 of proximal His-175. This conclusion was inferred from the significantly lowered value of the iron–imidazole stretching frequency of the mutant enzyme in its Fe(II) state (Smulevich et al., 1988a). Additional resonance Raman studies of the Fe(III) D235N mutant (Smulevich et al., 1988a) demonstrated that the Asp-235 → Asn mutation also has dramatic effects on the coordination behavior of the heme iron. This work showed that the ferric iron of the D235N mutant exists entirely in hexacoordinated form over the pH range 4.5–7.0; the CCP(MI) parent enzyme is largely pentacoordinated over this same pH range. Thus, the spectroscopic information demonstrates that the mutation results in a much-enhanced interaction between the ferric heme iron and the distal aquo ligand. As described below, these results are corroborated by the present crystallographic work.

Preliminary analysis of the mutant's enzyme activity shows that its steady-state rate of peroxide-dependent ferrocytochrome *c* oxidation is reduced (J. M. Mauro, unpublished results). Which step in the reaction pathway has been impeded most is unknown, but both the rate and pH dependence of oxidation of the enzyme by $H_2O_2$ and the kinetics of its subsequent reduction by ferrocytochrome *c* have been affected (J. M. Mauro and J. E. Erman, unpublished observations; also, see below).

*Crystal Structure of CCP(MI,D235N).* From the present 2.2-Å X-ray data for the mutant enzyme, a $F_o$(D235N) − $F_o$(parent) difference map revealed that structural changes occur on both the proximal and distal sides of the heme plane as a result of the Asp-235 → Asn replacement. When contoured at the ±3.5σ level (Figure 4a), the map showed features around the iron/distal coordination site as well as difference density on the proximal side of the heme near the mutated 235 position, in the region encompassing the side chains of Met-172, Met-230, Trp-191, and buried Wat-535.

The largest distal feature in the difference Fourier map (+10σ) was located very near the iron and was interpreted as being due to the presence of a ligand (assumed to be a water molecule or hydroxide ion) closely bound to the ferric heme iron as well as to movement of the iron toward the distal domain. No significant difference density was observed near Arg-48, His-52, Trp-51, or any other residues on the distal side. On the heme proximal side, the difference map showed unusual features near Trp-191 (Figure 4a). A strong negative peak (the most negative in the map, −11σ) was seen centered on the five-membered portion of a superimposed model of the parent Trp-191 indole ring. This negative difference density was bracketed by positive peaks (6.5σ) on both sides. These features provided a challenge during least-squares refinement with regard to proper assignment of the orientation of the indole ring of Trp-191, as described below. [See also Refinement of CCP(MI) and Mutant Structures.]

At a low contour level (±3.5σ), difference density features in the iron vicinity resemble those previously observed in the difference density map of peroxide-oxidized bakers' yeast CCP (compound I) minus resting state ferric CCP [$F_o$(compound I) − $F_o$(parent)] (Edwards et al., 1987). By analogy with the compound I structure, this pattern of difference density, consisting of a negative peak beneath the iron and other small peaks near His-175, suggested that movement of the iron/His-175 unit toward the distal side had occurred in the mutant. Finally, other small difference features (3.5σ) appeared on the heme proximal side near Met-172 and Met-230, as well as near buried water molecule 535.

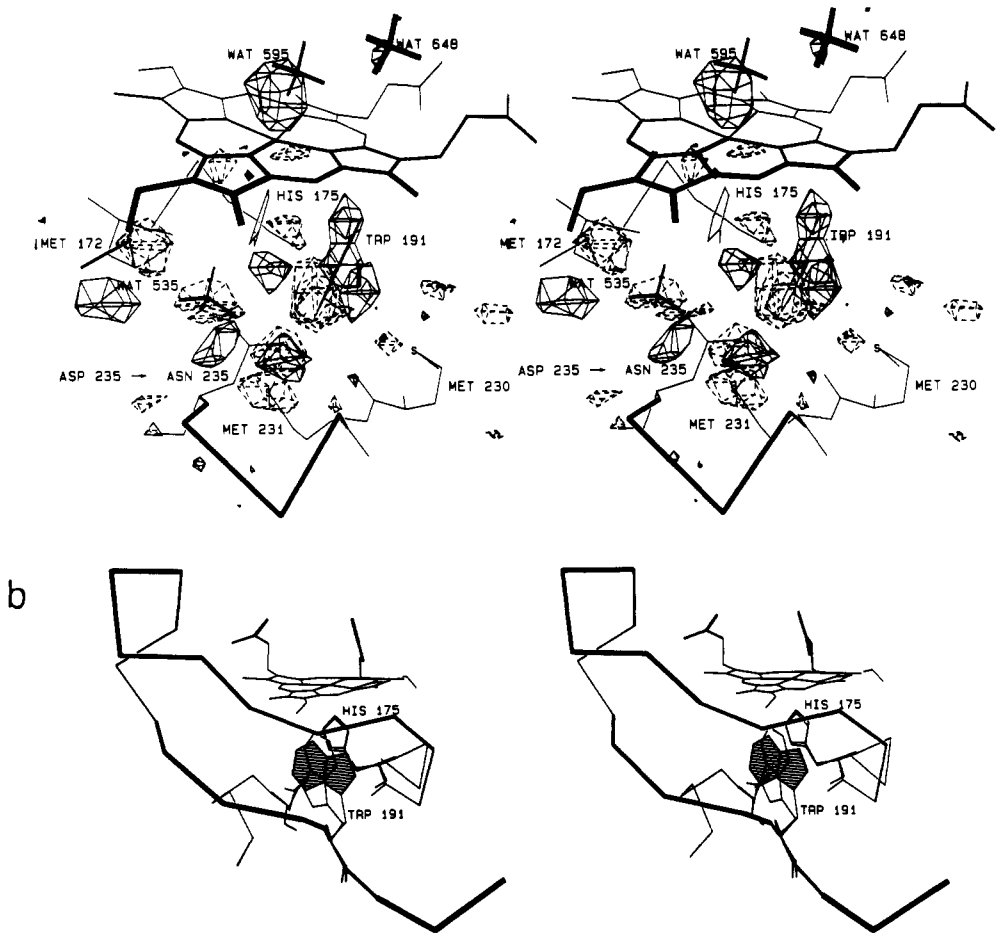


FIGURE 4: (a) CCP(MI,D235N) minus CCP(MI) difference Fourier map contoured at $\pm 3.5\sigma$. (b) Superposition of refined structures of CCP(MI,D235N) and CCP(MI). The indole ring of Trp-191 in its new orientation in the mutant is shown shaded.

Subsequent least-squares refinement of the D235N mutant enzyme structure showed that distal water 595 is displaced toward the heme plane by ca. 0.6 Å when compared to its position in the parent enzyme, while the heme iron is shifted upward (toward the distal side) by ca. 0.2 Å. The exact position of the iron relative to the pyrrole N plane is difficult to assign with a high degree of confidence due to errors in assessing the positions of the pyrrole nitrogens at the present resolution; however, the difference map clearly showed that the iron has moved and is now positioned in or slightly above the plane formed by the four pyrrole nitrogen atoms. The distance of the iron to Wat-595 in D235N has thus decreased from 2.7 Å in the CCP(MI) parent to 1.9–2.0 Å in the Asn-substituted enzyme. The new Fe(III)–O distance in the mutant is similar to the corresponding Fe(III)–O distance in hexacoordinated sperm whale metMb (Takano, 1977; Powers et al., 1984).

Interestingly, two fixed water molecules on the heme distal side, which in addition to Wat-595 occupy the peroxide-binding pocket, become more ordered in the mutant. Temperature factors for water molecules 596 and 648 in the mutant are 24 and 25 Å$^2$, respectively, compared to values of 40 and 58 Å$^2$ found in CCP(MI). This indicates that the mutation on the *proximal* side has had the effect of increasing the rigidity of the water-filled pocket on the heme *distal* side. This is presumably a secondary effect of the strong interaction of the iron with Wat-595 being propagated throughout the hydrogen-bonded network linking these distal water molecules.

Although at the present 2.2-Å resolution the magnitudes of very small (<0.2 Å) structural changes are difficult to assess quantitatively, crystallographic refinement suggested that the upward adjustment of the iron in the mutant was accompanied by a small upward movement and slight twisting of His-175, resulting in approximately the same final iron–nitrogen bond length as in CCP(MI) (2.0 Å). Additionally, the refined mutant structure showed that Met-172 and Met-230 moved 0.3–0.4 Å away from His-175 and Trp-191, respectively. Since all four of these residues lie below the heme in close proximity to one another and to the mutation site, it is not surprising that the Asp-235 → Asn substitution results in structural adjustments at these positions. The movement of Met-172 is very likely linked to the disorder or decreased occupancy observed at the site of adjacent buried water 535, since this water molecule is in van der Waals contact with S$\delta$ of Met-172 and is also positioned to form a strong hydrogen bond (2.7 Å) with Asp-235 in the parent molecule. Readjustment of Met-230 might be expected to occur in response to the significant reorientation of the side chain of Trp-191 that occurs in the D235N mutant (see below), since its S$\delta$ atom resides in van der Waals contact with N$\epsilon$ of the Trp-191 indole ring in the CCP(MI) parent.

In initial refinement cycles, the atoms composing the indole side chain of Trp-191 had an unusual distribution of temperature factors, with some of the atoms having *B*-factors 2 times larger than other atoms of the bicyclic indole ring system. The Trp-191 side chain was therefore examined by running refinement cycles with the Trp-191 side-chain atoms initially removed in order to obtain a relatively unbiased picture of its orientation. In this way, it was determined that the best fit to the observed electron density required a new orientation for Trp-191 in the mutant, differing from the original one by rotations of 195° around its C$\beta$–C$\gamma$ bond and of −34° around

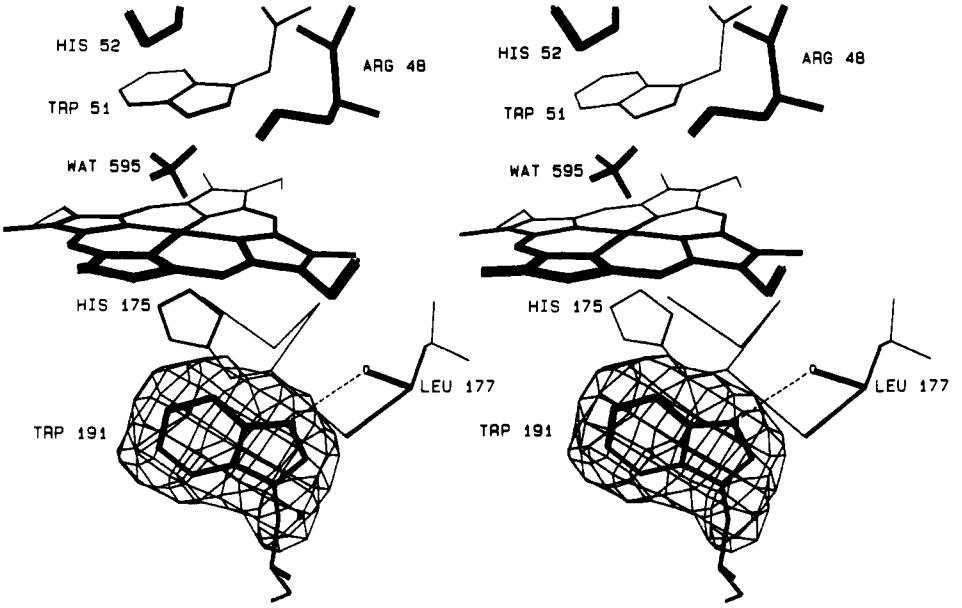


FIGURE 5: $F_o - F_c$ map, calculated after omitting Trp-191 coordinates, showing electron density fit to the reoriented Trp-191 side chain of CCP(MI,D235N). A newly formed hydrogen bond between Nε of the tryptophan and the backbone carbonyl oxygen of Leu-177 is indicated by the dashed line.

its Cα–Cβ bond. As shown in Figure 4b, the overall effect of these bond rotations is that the indole ring of Trp-191 in the mutant enzyme is flipped over and oriented very differently than the same ring is in the parent enzyme, with the long axis of the indole ring now nearly parallel with the porphyrin plane. In its new orientation, Nε of Trp-191 is now well positioned to form a hydrogen bond with the backbone carbonyl oxygen of Leu-177 (a 2.7-Å interaction) (Figure 5). In the parent enzyme, this backbone carbonyl oxygen atom is unusual in that it apparently exists in a non-hydrogen-bonded state in its position at the C-terminus of a distorted helix on the heme proximal side.

The new orientation assumed by Trp-191 in response to the Asp-235 → Asn substitution suggests the possibility that conformational flexibility of the protein in the region around Trp-191 may be functionally significant in the catalytic cycle of the parent enzyme. Essentially complete protonation of Asp-235 by His-175, whose acidity would be expected to increase upon formation of the oxyferryl compound I intermediate, may facilitate reorientation of the Trp-191 indole ring. Conceivably, interconversion of the two observed positions, or more likely, some less dramatic movement of this indole ring, could control the rate of intramolecular electron transfer between the protein-centered radical site and the heme iron (Ho et al., 1983). This idea is especially intriguing in light of recent evidence which suggests that the radical species in compound I is localized on the indole ring of Trp-191 (Mauro et al., 1988; Scholes et al., 1989; Sivaraja et al., 1989). We note that the largest proximal-side side-chain adjustment that occurs upon conversion of resting-state CCP to compound I occurs in the vicinity of Trp-191 (Edwards et al., 1987).

If the major protein-based radical species in compound I of CCP is indeed located on Trp-191, an important question is the extent to which the unusual magnetic properties of this oxidized center depend on the exact orientation of the indole ring. Since the newly-oriented indole ring of Trp-191 in CCP(MI,D235N) will have an altered set of interactions with adjacent buried side chains, especially with proximal His-175, EPR and ENDOR (electron nuclear double resonance) experiments may be of help in answering this question by examining the detailed electronic environment of any protein-based paramagnetic species produced upon reaction of the D235N mutant with $H_2O_2$.

Presumably, the new position of the iron relative to the porphyrin plane in the D235N mutant results from a relaxation of electronic restraints that fix the position of the iron–imidazole unit in the Asp-235-containing parent peroxidase. However, it is not possible from examination of the structure and properties of CCP(MI,D235N) to infer unambiguously the means by which Asp-235 acts in concert with the proximal histidine to affect the position and ligand-binding properties of the heme iron. This is because we cannot be completely certain that the changes in iron position and reactivity that have occurred are not secondary effects stemming from the reorientation of the indole ring of Trp-191 rather than being directly due to the changed local electrostatic environment that occurs as a result of the Asp-235 → Asn replacement. However, it seems unlikely that the changed orientation of the Trp-191 indole ring is responsible for the observed relaxation of the iron–imidazole unit toward the pyrrole plane, since the Trp-191 → Phe mutation resulted in no significant difference in the iron position compared with CCP(MI). Therefore, we tentatively conclude that the effective protonation state of iron-bound His-175 in its interaction with Asp- or Asn-235 is the primary factor controlling the iron's position and reactivity in CCP(MI) and its D235N mutant.

In a discussion of the results of resonance Raman studies on Fe(II) CCP(MI) and several of its mutants, we previously considered some of the factors that may regulate the degree of imidazolate character of His-175 and, in turn, the placement and reactivity of the heme iron (Smulevich et al., 1988a). The position of the proton shared by His-175 and Asp-235 appears to be of primary importance here. Due to the great disparity in $pK_a$ expected for Nδ1 of His-175 compared to Oδ1 of Asp-235, even after considering the likelihood of enhanced acidity of the Fe(II)-coordinated histidine, we were led to conclude that the most critical feature contributing to the rather surprising ability of His-175 to transfer a proton to Asp-235 is the isolation of these groups from bulk solvent. Neutralization of the buried negative charge of Asp-235 by means of proton transfer from the imidazole of His-175 serves to redistribute negative charge onto the imidazole, and the

resulting imidazolate anion is then partially neutralized by the Fe(II) center. The isolation of this proximal-side apparatus within the protein matrix apparently eliminates stabilization of carboxylate anion that would occur by multiple ion–dipole interactions with water molecules if Asp-235 were solvent-exposed.

The insulation of these proximal-side groups from contact with aqueous solvent very likely remains the dominant factor in determining the protonation state of Asp-235 relative to His-175 for *ferric* CCP(MI) and the mutant enzymes containing aspartate at position 235 whose X-ray structures are reported here, even though we expect there to be a somewhat greater tendency toward protonation of buried Asp-235 by His-175 than for the Fe(II) enzyme examined by resonance Raman spectroscopy. We base this conclusion on the work of Baldwin et al. (1986), who found a p$K_a$ of 10.5 for Fe(III)-coordinated His-18 of the proteolytic heme octapeptide (microperoxidase) from horse heart cytochrome *c*. Thus, assuming that the intrinsic p$K_a$ of His-175 coordinated to the Fe(III) heme in CCP approximates the value found for the microperoxidase model system, it seems clear that no significant degree of protonation of Asp-235, whose "normal" p$K_a$ is probably ca. 4.5, would be expected to occur in the absence of the solvent isolation phenomenon. In considering the protonation state of His-175 in the ferric D235N mutant, the situation is quite different. In this case there would appear to be no great driving force for protonation of the amide oxygen of Asn-235, since no buried charge need be neutralized. Furthermore, in view of the large difference in basicity of carboxylate compared to amide oxygen, it would not be surprising if Nδ1 of His-175 fails to transfer a proton to the amide oxygen of Asn-235 to any significant extent in this mutant, even supposing that the asparagine is properly oriented for such a transfer to occur.

Which of the two alternative orientations of the side-chain carboxamide group predominates in the D235N mutant remains an interesting unresolved question. This is because the side-chain atoms of Asn-235 occupy virtually the same space as the Asp-235 side chain atoms do in the parent enzyme, and it is impossible to assign the orientation on the basis of electron density maps. However, this type of structural question can often be approached by using supplementary evidence combined with chemical reasoning. In the present case, resonance Raman spectra (Smulevich et al., 1988a) show that the Fe(II)–N(imidazole) stretching frequency observed at 240 $cm^{-1}$ for Fe(II) CCP(MI) (and for CCP isolated from bakers' yeast) shifts to a much lower frequency, 205 $cm^{-1}$, for the ferrous D235N mutant. This decrease in stretching frequency was taken as evidence that Nδ1 of His-175 exists in the *non-hydrogen-bonded* and essentially fully protonated form in the Asn-235-substituted Fe(II) mutant. In interpreting the resonance Raman experiments, it was reasoned that if Nδ1 of His-175 in the Fe(II) D235N mutant exists hydrogen-bonded to the carboxamide oxygen of Asn-235 then the Fe(II)–N(imidazole) stretching frequency would be expected to be similar to the 220-$cm^{-1}$ value observed for deoxyMb, in which it is known that the proximal histidine is hydrogen-bonded to a backbone carbonyl oxygen atom (Bernstein et al., 1977). Instead, the Fe(II)–N(imidazole) stretching frequency of 205 $cm^{-1}$ obtained for this mutant is closer to that observed for Fe(II) porphyrin coordinated with non-hydrogen-bonded 2-methylimidazole dissolved in solvents such as benzene or methylene chloride (Stein et al., 1980; Hori & Kitagawa, 1980; Teraoka & Kitagawa, 1981). Thus, on the basis of this interpretation of the spectroscopic results, it seems likely that the side-chain carboxamide function of Asn-235 is oriented so that its oxygen is not available to hydrogen-bond with Nδ1 of His-175. If this is true, the carboxamide oxygen atom must face Trp-191, and the Asn-235 amide -$NH_2$ function must face Nδ1 of His-175, in the position previously occupied by carboxyl Oδ1 of Asp-235 in the parent peroxidase.

However, if the above orientation for Asn-235 is correct, and the oxygen atom of the side-chain carboxamide moiety of Asn-235 is available as a potential hydrogen-bond acceptor for the -NH hydrogen donor of the Trp-191 indole ring, it is not clear why the indole ring becomes completely reoriented so that a new hydrogen bond between Leu-177 and Nε of the indole is formed. One explanation for this is that orientation of Asn-235 inferred above on the basis of spectroscopic observations is incorrect; i.e., the carboxamide oxygen atom of Asn-235 is not available to hydrogen-bond with the Trp-191 indole ring because it is in fact occupied in a hydrogen-bonded interaction with Nδ1 of proximal His-175. This would leave the side-chain -$NH_2$ of Asn-235, a hydrogen donor, facing position 191, and it is reasonable that the indole position would readjust to avoid juxtaposition of two hydrogen donors (i.e., the -$NH_2$ of Asn-235 and the NεH of the indole) while retaining stabilization energy by forming a new hydrogen bond with Leu-177. In this context it is important to recall that the orientation of Asn-235 inferred above is based on this mutant's *Fe(II)–N(imidazole)* stretching frequency compared to the corresponding frequency for deoxyMb, and the possibility exists that myoglobin is simply not a good model for these proximal-side interactions in *ferric cytochrome c peroxidase*. Furthermore, on the basis of the expected acidity of the imidazole of His-175 compared to the acidity of the side-chain amide oxygen of Asn-235 discussed earlier, it is not clear that one would expect any appreciable degree of proton sharing (i.e., hydrogen bonding) to occur between the two groups even if they are properly juxtaposed in the mutant enzyme.

Of course, it is possible that the orientation for Asn-235 in CCP(MI,D235N) proposed on the basis of the resonance Raman results is correct and that the indole ring of Trp-191 flips over for reasons unrelated to stabilization energy gained by means of formation of a new hydrogen bond with Leu-177 in lieu of the hydrogen-bonded interaction between Asp-235 and Trp-191 that exists in the parent enzyme. This could be the case if subtle changes in ion–dipole, dipole–dipole, van der Waals, and hydrophobic forces are of more importance here than stabilization energy gained by hydrogen-bonding interactions. The question of the orientation of Asn-235 in the D235N mutant and the role it plays, if any, in determining the position of the side chain of Trp-191 remains open.

It has been asserted that Asp-235 very likely exerts a stabilizing influence on the oxyferryl center of compound I (Poulos & Finzel, 1984; Hashimoto et al., 1986). However, we have observed that CCP(MI,D235N) reacts with hydrogen peroxide to yield a product with a quite stable Fe(IV)=O center (J. M. Mauro, unpublished observations). Thus, it appears that the imidazolate character imparted to the proximal histidine as a result of its interaction with Asp-235 does not exert a major stabilizing effect on the oxyferryl center of the enzyme. It is our experience, rather, that mutations on the heme *distal* side (e.g., Trp-51 → Phe) have a much greater deleterious effect on the stability of the oxyferryl center (Fishel et al., 1987; J. M. Mauro, unpublished observations), although we can offer no simple explanation for this behavior at the present time.

What then is the role of Asp-235 in the enzymic function of cytochrome *c* peroxidase? At least a partial answer to this

question can now be given, as two likely functions for Asp-235 are clear from the D235N X-ray structure. First, this aspartate is apparently a necessary component in the apparatus by which the position of the ferric iron with respect to the porphyrin pyrrole plane in the resting-state enzyme is fixed, since the present Asp → Asn replacement results in a mutant enzyme in which the iron is readily able to remove into the heme plane and to interact strongly with either water or hydroxide at its sixth coordination site. This behavior of the D235N mutant is in contrast to that of the parent peroxidase, in which the resting-state iron is retracted at least 0.2 Å from the porphyrin plane and exists largely in pentacoordinate form. A second proposed role of Asp-235, based on the present D235N structure, is to assure proper positioning of the indole ring of Trp-191 by hydrogen-bond formation between its Oδ2 and Nε of the tryptophan. Although the importance of the exact position of the indole ring of Trp-191 to the function of the enzyme remains unknown, there is a growing body of evidence pointing to Trp-191 as a key element in both compound I stabilization and electron transfer from ferrocytochrome *c* (Mauro et al., 1988; Edwards et al., 1987, 1988; Sivaraja et al., 1989; Erman et al., 1989).

*Implications of the Present Structural Analyses for the Mechanism of Peroxide Binding to CCP.* It has been convincingly demonstrated that the heme iron in ferric cytochrome *c* peroxidase is essentially pentacoordinated (Finzel et al., 1984; Hashimoto et al., 1986; Smulevich et al., 1988a; Dasgupta et al., 1989; the present work); thus, it is obvious that the enzyme has evolved the structural means to restrict access of aquo ligands to the sixth iron coordination site while still allowing extremely rapid reaction (ca. $10^7$ $M^{-1}$ $s^{-1}$) with peroxide substrates (Loo & Erman, 1975). Both proximal and distal structural features contribute to the maintenance of the pentacoordinate resting-state iron. On one side of the heme, strong interaction of the iron with coordinated His-175 keeps the iron removed about 0.2 Å from the pyrrole plane. The strength of the iron–His-175 interaction is enhanced by increased imidazolate character imparted to the histidine by means of its hydrogen-bonding interaction with buried Asp-235. Strong iron–His-175 π-orbital interaction probably also serves to make the iron less reactive at the remaining sixth coordination site. On the opposite side of the heme, a web of hydrogen bonds linking loosely-fixed distal water molecules and the side chains of Trp-51, His-52, and Arg-48 keeps axial water 595 suspended at a distance too far for significant interaction with the iron to occur. Removal of one of these H-bonds by a Trp-51 → Phe substitution results in an enzyme with hexacoordinate high-spin iron (in the absence of MPD) and underscores the delicate balance of forces at play in this distal pocket. Thus, unlike hexacoordinated metMb, the iron in resting-state CCP remains pentacoordinated. Furthermore, the tendency of the enzyme's ferric iron to bind hydroxide under basic conditions is probably retarded by these same features, allowing the enzyme to rapidly react with peroxide over a wide range of pH.

The effective maintenance of pentacoordinated iron in the ferric resting-state enzyme obviates the need for peroxy anion, generated as a result of deprotonation of incoming hydroperoxide by distal His-52 (Poulos & Kraut, 1980a), to either directly displace or await dissociation of an iron-coordinated aquo ligand before reacting with the iron. Thus, highly nucleophilic $HO_2^-$ (Edwards & Pearson, 1962) need only displace loosely-bound heme-cleft water molecules prior to, or in concert with, its attack on the iron.

Preliminary stopped-flow experiments conducted to investigate the consequences of enhanced ligand-binding ability of the ferric D235N mutant indicate that the rate of reaction of the D235N mutant with $H_2O_2$ is rapid and proportional to oxidant concentration below pH 6, but the reaction then becomes much slower and *independent* of peroxide concentration above this pH (J. E. Erman, unpublished results). In contrast, the rate of reaction of the parent enzyme with peroxide remains rapid (ca. $10^7$ $M^{-1}$ $s^{-1}$) and proportional to peroxide concentration over the pH range 5–8 (Loo & Erman, 1975). The results of resonance Raman studies of the ferric D235N mutant indicate that at low pH it is likely that water is the relatively loosely coordinated high-spin sixth ligand, while above pH 6 hydroxide ion is probably the strongly bound low-spin sixth ligand (Smulevich et al., 1988a). Thus, the change in the mutant's kinetic behavior as a function of pH may be due to binding of hydroxide ion that occurs above pH 6. At low pH, peroxy anion should be able to displace high-spin water relatively easily; however, under more basic conditions, the substrate anion cannot effectively compete at the sixth coordination site with the more basic hydroxide ion. In this case, then, hydroperoxide anion would be forced to await dissociation of hydroxide before reacting at the iron center, leading to the observed kinetics.

## ACKNOWLEDGMENTS

We thank Dr. G. Smulevich, Dr. T. G. Spiro, Dr. J. Terner, and Dr. J. E. Erman for access to their results prior to publication. We express our gratitude to the San Diego Supercomputer Center for generously providing computing time.

**Registry No.** CCP, 9029-53-2.

## REFERENCES

Altschul, A. M., Abrams, R., & Hogness, T. R. (1940) *J. Biol. Chem. 136*, 777–794.

Baldwin, D. A., Marques, H. M., & Pratt, J. (1986) *J. Inorg. Biochem. 27*, 245–254.

Bernstein, F. C., Koetzle, T. F., Williams, G. J. B., Meyer, E. F., Jr., Brice, M. D., Rodgers, J. R., Kennard, O., Shimanouchi, T., & Tasumi, M. (1977) *J. Mol. Biol. 112*, 535–542.

Bolin, J. T., Filman, D. J., Matthews, D. A., Hamlin, R. C., & Kraut, J. (1982) *J. Biol. Chem. 257*, 13650–13662.

Chance, B., Devault, D., Legallais, V., Mela, L., & Yonetani, T. (1967) in *Fast Reactions and Primary Processes in Chemical Kinetics* (Claesson, S., Ed.) pp 437–464, Interscience, New York.

Chance, M., Powers, L., Poulos, T., & Chance, B. (1986) *Biochemistry 25*, 1266–1270.

Crowther, R. A. (1972) in *The Molecular Replacement Method* (Rossmann, M. G., Ed.) pp 173–178, Gordon and Breach, New York.

Crowther, R. A., & Blow, D. M. (1967) *Acta Crystallogr. 23*, 544–548.

Dasgupta, S., Rousseau, D. L., Anni, H., & Yonetani, T. (1989) *J. Biol. Chem. 264*, 654–662.

Edwards, J. O., & Pearson, R. G. (1962) *J. Am. Chem. Soc. 84*, 16–24.

Edwards, S. L., Xuong, Ng.-h., Hamlin, R. C., & Kraut, J. (1987) *Biochemistry 26*, 1503–1511.

Erman, J. E. (1974) *Biochemistry 13*, 39–44.

Erman, J. E., & Yonetani, T. (1975) *Biochim. Biophys. Acta 393*, 350–357.

Erman, J. E., Vitello, L. B., Mauro, J. M., & Kraut, J. (1989) *Biochemistry 28*, 7992–7995.

Finzel, B. C., Poulos, T. L., & Kraut, J. (1984) *J. Biol. Chem. 259*, 13027–13036.
Fishel, L. A., Villafranca, J. E., Mauro, J. M., & Kraut, J. (1987) *Biochemistry 26*, 351–360.
George, P., Hanania, G. I. H., Irvine, D. H., & Abbu-Issa (1964) *J. Chem. Soc.*, 5689–5694.
Goltz, S., Kaput, J., & Blobel, G. (1982) *J. Biol. Chem. 257*, 11186–11190.
Goodin, D. B., Mauk, A. G., & Smith, M. (1986) *Proc. Natl. Acad. Sci. U.S.A. 83*, 1295–1299.
Goodin, D. B., Mauk, A. G., & Smith, M. (1987) *J. Biol. Chem. 262*, 7719–7724.
Hashimoto, S., Teraoka, J., Inubushi, T., Yonetani, T., & Kitagawa, T. (1986) *J. Biol. Chem. 261*, 11110–11118.
Hayashi, Y., & Yamazaki, T. (1979) *J. Biol. Chem. 254*, 9101–9106.
Hendrickson, W. A., & Konnert, J. H. (1980) in *Computing in Crystallography* (Diamond, R., Ramaseshan, S., & Venkatesan, K., Eds.) pp 13.1–13.23, Indian Institute of Science, Bangladore, India.
Ho, P. S., Hoffman, B. M., Kang, C. H., & Margoliash, E. (1983) *J. Biol. Chem. 258*, 4356–4363.
Hoffman, B. M., Roberts, J. E., Brown, T. G., Kang, H. K., & Margoliash, E. (1979) *Proc. Natl. Acad. Sci. U.S.A. 76*, 6132–6136.
Hoffman, B. M., Roberts, J. E., Kang, C. H., & Margoliash, E. (1981) *J. Biol. Chem. 256*, 6556–6564.
Hori, H., & Kitagawa, T. (1980) *J. Am. Chem. Soc. 102*, 3608–3613.
Hori, H., & Yonetani, T. (1985) *J. Biol. Chem. 260*, 349–355.
Jones, T. A. (1978) *J. Appl. Crystallogr. 11*, 268–272.
Kaput, J., Goltz, S., & Blobel, G. (1982) *J. Biol. Chem. 257*, 15054–15058.
Loo, S., & Erman, J. E. (1975) *Biochemistry 14*, 3467–3470.
Luzzati, V. (1952) *Acta Crystallogr. 5*, 802–810.
Mauro, J. M., Fishel, L. A., Hazzard, J. T., Meyer, T. E., Tollin, G., Cusanovich, M. A., & Kraut, J. (1988) *Biochemistry 27*, 6243–6255.
Mauro, J. M., Miller, M. A., Edwards, S. L., Wang, J., Fishel, L. A., & Kraut, J. (1989) in *Metals Ions in Biological Systems 25* (Sigel, H., & Sigel, A., Eds.) pp 477–503, Marcel Dekker, New York and Basel, Switzerland.
Mazza, G., & Welinder, K. G. (1980) *Eur. J. Biochem. 108*, 481–489.
Meyer, R., Ha, T.-K., & Gunthard, Hs. H. (1975) *Chem. Phys. 9*, 393–402.
Miller, M. A., Hazzard, J. T., Mauro, J. M., Edwards, S. L., Simons, P. C., Tollin, G., & Kraut, J. (1988) *Biochemistry 27*, 9081–9088.
Murthy, M. R. N., Reid, T. J., Sicignano, A., Tanaka, N., & Rossmann, M. G. (1981) *J. Mol. Biol. 152*, 465–499.
Poulos, T. L., & Kraut, J. (1980a) *J. Biol. Chem. 255*, 8199–8205.
Poulos, T. L., & Kraut, J. (1980b) *J. Biol. Chem. 255*, 10322–10330.
Poulos, T. L., & Finzel, B. C. (1984) *Pept. Protein Rev. 4*, 115–171.
Poulos, T. L., Freer, S. T., Alden, R. A., Xuong, Ng.-h., Edwards, S. L., Hamlin, R. C., & Kraut, J. (1978) *J. Biol. Chem. 253*, 3730–3735.
Poulos, T. L., Freer, S. T., Alden, R. A., Edwards, S. L., Skogland, U., Takio, K., Eriksson, B., Xuong, Ng.-h., Yonetani, T., & Kraut, J. (1980) *J. Biol. Chem. 255*, 575–580.
Powers, L., Sessler, J., Woolery, C., & Chance, B. (1984) *Biochemistry 23*, 239–244.
Rossmann, M. G., & Blow, D. M. (1962) *Acta Crystallogr. 15*, 24–31.
Satterlee, J. D., Erman, J. E., LaMar, G. N., Smith, K. M., & Langry, K. C. (1983) *J. Am. Chem. Soc. 105*, 2099–2104.
Scheidt, W. R., & Gouterman, M. (1983) in *Iron Porphyrins I* (Lever, A. B. P., & Gray, H. B., Eds.) pp 89–139, Addison-Wesley, Reading, MA.
Scholes, C. P., Liu, Y., Fishel, L. A., Farnum, M. F., Mauro, J. M., & Kraut, J. (1989) *Isr. J. Chem. 29*, 85–92.
Sheriff, S., & Hendrickson, W. A. (1987) *Acta Crystallogr. A34*, 118–121.
Sitter, A. J., Reczek, C. M., & Terner, J. (1985) *J. Biol. Chem. 260*, 7515–7522.
Sivaraja, M., Goodin, D. B., Smith, M., & Hoffman, B. M. (1989) *Science 245*, 738–740.
Smulevich, G., Mauro, J. M., Fishel, L. A., English, A. M., Kraut, J., & Spiro, T. G. (1988a) *Biochemistry 27*, 5477–5485.
Smulevich, G., Mauro, J. M., Fishel, L. A., English, A. M., Kraut, J., & Spiro, T. G. (1988b) *Biochemistry 27*, 5486–5492.
Smulevich, G., Wang, Y., Mauro, J. M., Wang, J., Fishel, L. A., Kraut, J., & Spiro, T. G. (1990) *Biochemistry* (following paper in this issue).
Stein, P., Mitchell, M., & Spiro, T. G. (1980) *J. Am. Chem. Soc. 102*, 7795–7797.
Takano, T. (1977) *J. Mol. Biol. 110*, 537–568.
Takio, K., Titani, K., Ericsson, L. H., & Yonetani, T. (1980) *Arch. Biochem. Biophys. 203*, 615–629.
Teraoka, J., & Kitagawa, T. (1981) *J. Biol. Chem. 256*, 3969–3977.
Thaller, C., Weaver, L. H., Eichele, G., Wilson, E., Karlsson, R., & Jansonius, J. N. (1981) *J. Mol. Biol. 147*, 465–469.
Tien, M., & Tu, C.-P.D. (1987) *Nature 326*, 520–523.
Wang, J. (1988) Ph.D. Dissertation, University of California, San Diego.
Welinder, K. G. (1976) *FEBS Lett. 72*, 19–23.
Welinder, K. G., & Mazza, G. (1977) *Eur. J. Biochem. 73*, 353–358.
Xuong, Ng.-h., Nielson, C., Hamlin, R., & Anderson, D. H. (1985a) *J. Appl. Crystallogr. 18*, 342–350.
Xuong, Ng.-h., Sullivan, D., Nielson, C., & Hamlin, R. (1985b) *Acta Crystallogr. B41*, 267–269.
Yonetani, T. (1971) in *Probes of Structure and Function of Macromolecules and Membranes II* (Chance, B., Yonetani, T., & Mildvan, A., Eds.) pp 545–552, Academic Press, New York.
Yonetani, T., & Ray, G. S. (1965) *J. Biol. Chem. 240*, 4503–4508.
Yonetani, T., & Ray, G. S. (1966) *J. Biol. Chem. 241*, 700–706.
Yonetani, T., Schleyer, H., & Ehrenberg, A. (1966a) *J. Biol. Chem. 241*, 3240–3243.
Yonetani, T., Wilson, D. F., & Seamonds, B. (1966b) *J. Biol. Chem. 241*, 5347–5352.